Hierarchical Bitmask Implicit Grids for Efficient Point-in-Volume Queries on the GPU

Julius Ikkala[a], Tuomas Lauttia[b], Pekka Jääskeläinen[c] and Markku Mäkitalo[d]
Tampere University, Tampere, Finland
fi

Keywords: Computer Graphics, Real-Time Rendering, Ray Tracing, Data Structures.

Abstract: We propose "Hierarchical Bitmask Implicit Grids", a novel, memory-efficient spatial index data structure for querying bounding volumes based on a contained point, targeting real-time use cases on GPUs. Like grid structures based on 3D arrays, implicit grids allow for nearly array-like direct lookups of cells without traversal through a spatial tree structure. However, the space complexity of this structure is $O(n)$ with respect to resolution as opposed to $O(n^3)$, which allows for dramatically higher resolutions than would be feasible with a 3D array. We demonstrate the effectiveness of this data structure by applying it to two example use cases: light culling and decal rendering. We measure both cases with ray tracing and multi-view rendering. We show that with tens of thousands of entries, our data structure can be built in 0.1–0.2 milliseconds, being $\sim$2.9x faster than the compared state-of-the-art decal method and orders of magnitude faster than dense 3D arrays, while delivering at least similar or even up to doubled rendering performance.

1 INTRODUCTION

Looking up overlapping volumes for a point in space is a common problem in real-time computer graphics. Two typical examples of this encountered in modern video games are light culling, i.e. figuring out which limited set of lights are taken into account when shading a surface; and decals, which modify the material data at a surface in order to add things like bullet holes and puddles, often dynamically. (Akenine-Möller et al., 2018)

These problems are typically solved with highly efficient screen-space structures (Olsson and Assarsson, 2011; Geffroy et al., 2020). However, the screen-space domain does not include points outside of the view frustum, which are commonly encountered with ray tracing, as rays can freely bounce within the scene. For multi-view displays, screen-space structures would be calculated for each view separately, multiplying their build time by however many views are needed. For example, the Looking Glass Portrait display usually takes between 48–100 separate views in its "quilt" (Looking Glass Factory, Inc., 2023). Even a 0.1 ms build time for a single view can therefore balloon to 5 to 10 milliseconds, which is a significant portion of the 16 milliseconds available in a 60 Hz target framerate.

Both issues with ray tracing and multi-view displays can be alleviated by using a world-space data structure. Several contemporary game engines are using grids based on 3D arrays (Unity Technologies, 2023; Kelly et al., 2021) to cull light sources for ray tracing. These have fast lookup times: the lookup is simply accessing an array, unlike tree structures, which traverse through a hierarchy of nodes with data dependencies between each step. The downside to 3D arrays is the space complexity of $O(n^3)$, which makes high-resolution or large-scale grids impractical. Varying grid cell sizes based on camera distance alleviates this problem somewhat in practice (Kelly et al., 2021), at the expense of precision at distance.

As an improvement over 3D arrays, we propose a world-space data structure for querying a list of volumes overlapping with a given point in space. It is an implicit grid; the cells are only constructed during lookup by combining per-axis information. The implicit grid is sliced into slabs along each of the three principal axes. The overlap status of each entry's volume is stored in a bitmask with each slab. Given a point, taking the bitwise AND of the bitmasks of corresponding slabs yields a set of overlapping volumes with no false negatives.

[a] https://orcid.org/0000-0002-5373-3190
[b] https://orcid.org/0000-0003-3568-6316
[c] https://orcid.org/0000-0001-5707-8544
[d] https://orcid.org/0000-0001-8164-0031

Ikkala, J., Lauttia, T., Jääskeläinen, P. and Mäkitalo, M.
Hierarchical Bitmask Implicit Grids for Efficient Point-in-Volume Queries on the GPU.
DOI: 10.5220/0012421600003660
Paper published under CC license (CC BY-NC-ND 4.0)
In *Proceedings of the 19th International Joint Conference on Computer Vision, Imaging and Computer Graphics Theory and Applications (VISIGRAPP 2024) - Volume 1: GRAPP, HUCAPP and IVAPP*, pages 285-292
ISBN: 978-989-758-679-8; ISSN: 2184-4321
Proceedings Copyright © 2024 by SCITEPRESS – Science and Technology Publications, Lda.

The bitmasks are very sparse when there are thousands of small volumes in a large scene. To take advantage of this sparsity, we propose a hierarchical layer which allows skipping over large empty portions in the bitmasks, improving lookup time significantly. With the bitmask sizes we suggest, just one layer of hierarchy is effective for up to at least tens of thousands of entries. We further increase the effectiveness of this hierarchical structure by sorting the entry volumes along the Z-order curve (Morton, 1966) before building the acceleration structure.

In practice, we demonstrate that on contemporary GPU hardware, this data structure is efficient to build from scratch, even with up to tens of thousands of entries. Further, we show that our data structure is highly effective for its typical use cases: light culling and decal lookup in multi-view rasterization and ray tracing. In this article, we present the following contributions:

- Application of implicit grids to light culling in ray tracing and multi-view contexts.
- Application of implicit grids to decal rendering in ray tracing and multi-view contexts.
- Addition of a hierarchical layer and Z-order curve sorting to implicit grids for improving the lookup performance.

2 RELATED WORK

Tiled Deferred Shading and *Tiled Forward Shading* (Balestra and Engstad, 2008; Olsson and Assarsson, 2011) cull lights with a contribution below a given threshold by dividing the screen into tiles and assigning the kept lights to each tile. Clustered deferred and forward shading (Olsson et al., 2012) improve on this by presenting a method that also divides the tile frusta into cells (called *clusters*) by depth. Compared to tiled shading, this method lets fewer lights be handled within screen-space tiles with great depth discontinuities. Similar data structures have also been used for decal rendering in forward pipelines (Geffroy et al., 2020). However, these screen-space structures are not generally applicable to ray tracing, as they only cull data within the viewport, while bounced rays can reach out-of-screen areas as well. Multi-view rendering would also require building these for each viewpoint, making the build time of screen-space structures less than ideal in that case.

World-space light clustering methods have been limited to naive dense grids in the industry (Unity Technologies, 2023; Kelly et al., 2021). The cubic space complexity of these grids forces them to be quite low-resolution. (Kelly et al., 2021) uses varying cell sizes in the grid structure, based on camera position. We use uniform cell sizes, as the implicit data structure allows for enough precision with a compact memory footprint to simply increase resolution globally whenever precision is not high enough near the camera.

(Bahnassi, 2021) present methods for finding decals in world-space by placing their bounding volumes in a Top-Level Acceleration Structure (TLAS) and tracing effectively zero-length rays. Their most performant variant that supports multiple overlapping decals is based on using an any-hit shader to collect a list of decals. They suggest using a small array for this, e.g. 2-3 entries. Having more overlapping decals than that will cause issues with this method, appearing as unpredictable decal ordering and missing decals. They also present a variant which does not have this limitation, but it is an order of magnitude slower according to their measurements.

Our proposed method has similarities to collision detection methods: the *sweep-and-prune* algorithm (also known as *sort-and-sweep*) (Baraff, 1992) uses a similar approach in which objects are bound by overlapping slabs along axes. However, that method divides the axes continuously and cannot do individual coverage lookups in constant time. The basic bitmask-based implicit grid data structure itself is not new: (Ericson, 2005) introduced a form of it for use in collision detection (*implicit grid using bit arrays*).

Another data structure with similarities has been proposed in the context of light culling for rasterization by (Drobot, 2017). Their light clustering method separates the Z axis from the X and Y axis with “Z-binning” and also uses bitmasks. Based on this, a blog post (Sylvan, 2017) suggested binning X and Y axes as well. This would have resulted in a similar data structure as the one described by (Ericson, 2005). However, the author admits in the post that they did not implement or evaluate the method.

To our knowledge, the implementation of this data structure in this field and the hierarchical layer are novel contributions. Compared to grids based on 3D arrays, implicit grids improve on the space complexity, from $O(n^3)$ to $O(n)$ where n is the number of grid cells along an edge. The hierarchical layer improves iteration speed in situations with tens of thousands of entries by allowing skipping large portions of the bitmask at once.

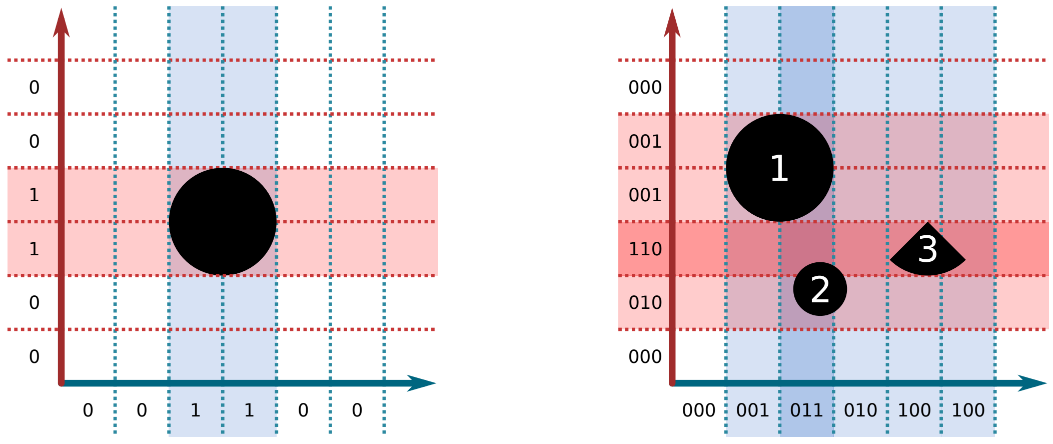

(a) One object. A set bit signals presence on a slab. (b) For multiple objects, there is one bit per object.

Figure 1: A 2D analog of the data structure. The bitmasks on each slab specify which objects overlap with the slab. The least significant bit corresponds to object 1. The bitwise-AND of the bitmasks of two slabs corresponding to any grid cell results in a bitmask representing the set of objects which potentially overlap with the cell.

3 IMPLICIT GRID

The proposed implicit grid data structure works by storing the effective range of each object along three axes. The axes are sliced into evenly spaced slabs. Each slab is represented by a bitmask. A slab bitmask has one bit per object, which is set to 1 if the object overlaps with this slab and 0 if not. To determine which objects overlap with a given grid cell in space, a bitwise AND of the bitmask of the corresponding slab on each axis is taken. The objects which potentially overlap with the grid cell are set to 1 in the resulting bitmask. Due to the nature of using three perpendicular axes in this data structure, the shape of the volume bounding an object is an axis-aligned rectangular cuboid, so the structure will report false positives if the true shape of the range is something else. Figure 1a visualizes the implicit grid with a single object, while Figure 1b shows a multi-object situation.

Compared to explicit grids, this method is both cache friendly and memory efficient (Ericson, 2005); the data needed to look up a grid cell is always near its world-space neighbors in memory as well, due to each axis being stored as a linear list of bitmasks. Additionally, the memory usage and build time is $O(3mn)$ instead of $O(mn^3)$, where m is the number of entries and n is the number slabs on every axis. Both benefits map well to modern GPU architectures as well.

In practice, we store the per-slab bitmask as an array of 4-channel vectors of 32-bit unsigned integers. We selected this vector width by also testing 2-channel 32-bit vectors and 4-channel 64-bit vectors, and found the 4-channel 32-bit approach fastest in our implementation, on an RTX 3090. Other sizes could very well be optimal on some other hardware or use cases. Since these parameters do not affect the output image in any way, the optimal parameters can be chosen by selecting whichever is fastest on the hardware in question. A 4-channel vector of 32-bit integers has 128 bits, and can thus represent the presence of 128 entries. We call these vectors “bitmask sectors” going forward.

Table 1: An example of a hierarchical bitmask layer, with sector size of 4 bits. The hierarchical layer can be used to quickly skip large portions of the full bitmask.

Entry indices	16-13	12-9	8-5	4-1
Full bitmask	0000	0000	1100	0101
Hierarchy layer	0	0	1	1

3.1 Hierarchy

Once the number of entries is high enough (typically in the tens of thousands), directly iterating through all bitmask sectors becomes costly. Most of the bitmask sectors are usually empty, as entries generally only cover a small portion of the entire scene. To reduce the number of reads needed to iterate through the set bits of the bitmask, we use another bitmask as a layer of hierarchy. The bits of this hierarchical bitmask layer represent each sector of the base bitmask. A bit is set to 1 if any of the bits in the corresponding sector is 1. This way, bitmask sectors fully consisting of zero can be quickly skipped. Table 1 shows an example case of this.

Even if the bitmasks are mostly sparse, if the order of entries is random, the bits are spread throughout the sectors uniformly, causing many bitmask sectors to have just a few bits set. The hierarchy is most effective when as many sectors as possible are fully zero and thus skippable, with the 1-bits mostly present together in individual sectors. Sorting the entries according to the Z-order curve (Morton, 1966) before building the implicit grid drastically improves the efficiency of the hierarchy, due to grouping nearby entries in the same or nearby bitmask sectors. Figure 2 visualizes the effect of this sorting.

We calculate the Z-order curve inside the axis-aligned bounding box (AABB) that contains the centroids of all objects, and sort based on the centroid location. We use 10-bit precision per axis in the curve, as it was the maximum precision we could fit in a 32-bit index (3 axes times 10 bits). Lower precision can also be used, but doing so can reduce the benefit gained by sorting when the resolution of the Z-order curve is lower than the density of slabs in the grid.

3.2 Building

The process of building the implicit grid consists of the following steps:

1. (Optional) Sort volumes by centroid coordinate along Z-order curve
2. Calculate applicable range of each volume along each axis
3. For each bitmask sector of each slab of each axis, find overlapping volume ranges and assign bits
4. (Optional) Build hierarchical bitmask layer based on high-resolution bitmasks.

The building process can be fully implemented on the GPU, and the steps past sorting are “embarrassingly parallel”.

We implement step 1 using a Vulkan-based radix sort implementation (The Fuchsia Authors, 2021). In practice, we used a 30-bit Z-order curve, 10 bits per axis. The curve is aligned to the AABB containing the centroids of all volumes. The sorting is used to roughly cluster lights with similar overlaps into successive bits; this makes the hierarchical bitmask layer more effective at skipping sectors due to more sectors being completely zero. If the hierarchical layer is not used, this specific benefit no longer applies and sorting can thus be skipped without major performance implications.

When handling step 2 in the light culling context, the range of each light is initially estimated based on a cut-off brightness parameter. During step 2, the structure can take visibility into account for a fairly low additional cost. If shadow maps have been computed for each light source, the ranges can be bounded by the maximum AABB of the distances present in each shadow map. Decals, on the other hand, are typically already defined as Oriented Bounding Boxes (OBB); the range step only needs to find the extents of the OBB along each grid axis (i.e. find the AABB containing the decal OBB).

For step 3, we use a workgroup geometry of 32×4, representing 32 slabs and the 4 32-bit unsigned integers forming a sector. Each work item reads one range into shared memory, corresponding to the 128 bits in the current sectors. This way, the range information needed to build the bitmasks for 32 slabs can be fetched at once. The rest of the step is trivial: on each slab, go through the light ranges for the sector, and write a 0 or 1 bit to the bitmask depending on if the range overlaps with the bitmask's slab.

Step 4, the hierarchical layer, is optional, and usually only beneficial when the number of entries is in the thousands. It is built in a quite simple manner: for each bit in the hierarchical layer, read the sector from the full bitmask, and check if it is non-zero.

3.3 Iterating over Entries

First, the queried point's coordinate is transformed and quantized to the location and resolution of the implicit grid. The resulting coordinates on each axis correspond directly to the slab indices. When not utilizing the hierarchical layer, we then iterate through the bitmasks of the selected slabs, calculate the bitwise AND between them, and report the index of each set bit as an overlap.

As a concrete example, in the decal rendering case, if the queried point is the position of the surface depicted in a given pixel, then the reported indices correspond to decals which are potentially present at the surface.

In the case with a hierarchy, we first iterate through the hierarchy bitmask in a similar bitwise AND fashion. Instead of reporting the index when a set bit is encountered, we instead now visit the corresponding sector in the underlying bitmask and calculate the bitwise AND between those slabs and report those indices.

4 EXPERIMENTAL SETUP

We apply the proposed hierarchical bitmask implicit grid (*HBIG*) data structure to two different use cases: decal rendering and light culling. In both situations, we use a PBR version of the “Sponza” scene (The Khronos Group, 2018) with added relevant elements, as shown in Figure 3. We set our implicit grid imple-

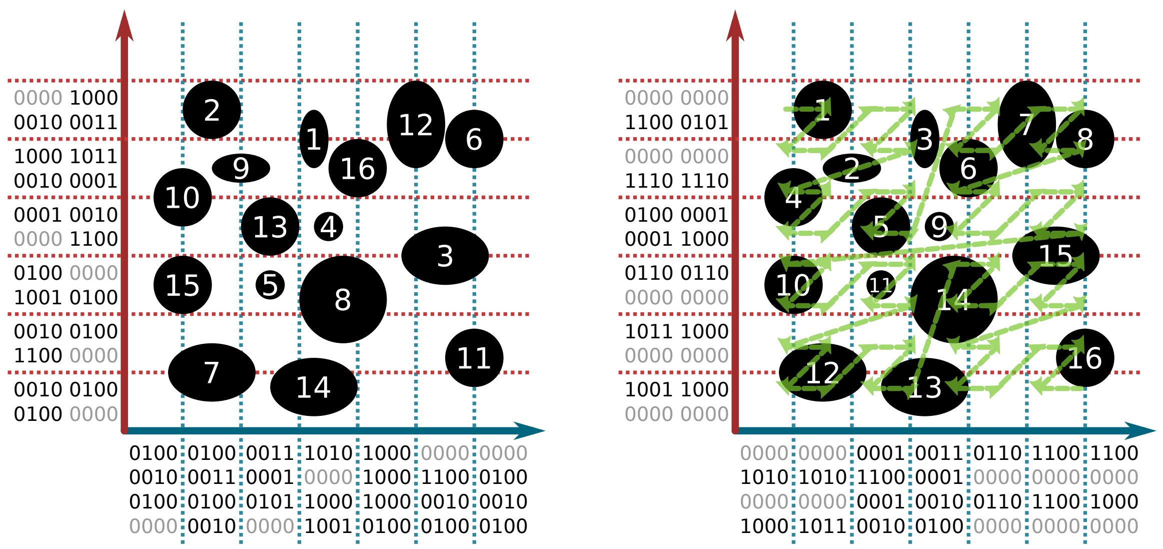

(a) The objects are in random order. (b) The new indices assigned along a Z-order curve.

Figure 2: A 2D analog of the data structure, showing bitmasks in a 16-object situation. In each bitmask, the top-left bit corresponds to object 16, while the bottom-right corresponds to 1. **(a)** The objects are in random order. As the indices for each bitmask are mostly uniformly distributed, it is rare for 4-bit sectors to be fully zero. **(b)** The indices have been assigned along the Z-order curve. As ordering the objects according to their location also places them near each other in the bitmask, they are more likely to appear in the same sector. This increases the number of empty sectors, which in turn lets the hierarchical bitmask layer skip more entries.

mentation to start using the hierarchy layer and entry sorting at 1024 entries, as they have little to no benefit before that. In all cases, we use a resolution of 512^3 for all implicit grids.

For decal rendering, we measure performance by spreading a range of 0 to 65536 decals across the surfaces of the test scene at random, as seen in Figure 3a. In this case, the scene is lit by one bright light source. We compare our method to a decal rendering method based on using the Top-Level Acceleration Structure (*TLAS*) for querying the bounding boxes of decal volumes (Bahnassi, 2021).

The TLAS approach requires special care with overlapping decals; to be performant, the maximum number of allowed overlapping decals needs to be fairly small. However, our test case has several regions with lots of overlaps. We set the maximum overlap count to 4 to not slow down the algorithm too much but also allow it to deal with many of the overlapping decals, although several areas in the scene still have some issues due to having 5 or more overlaps.

For light culling, we spread 0 to 65536 point lights randomly in the same scene, as seen in Figure 3b. The lights are kept relatively dim so that for any point in space, most lights can be culled. This is necessary to demonstrate the efficiency of light culling algorithms. We compare our method to 3D arrays with links to light lists. Constant-size cells were used due to the relatively constrained size of the scene. We present two cases: 16^3 (*A16*) which is faster to build but causes long light lists due to low granularity, and 32^3 (*A32*) which is slower to build but has more precision to cull lights more accurately.

For both use cases, we measure two contexts: multi-view rasterization and path tracing. For multi-view rasterization, we render a 16×8 grid of views at the resolution of 256×256, offset from each other by 0.1 units. This setup is chosen to approximate the needs of light field displays (Looking Glass Factory, Inc., 2023) while keeping rendering performance in the real-time territory. For ray tracing with decals, we path trace one indirect bounce at 1920×1080. For the light case, we instead calculate shadow rays to each shaded light, but only if the light is within its range. This approach limits the performance hit of false positives. We did not implement similar skipping in the multi-view case, which thus also visualizes the false positive rate differences more clearly.

In all cases, we measure the time taken to build the corresponding data structure, as well as rendering time. Build times include sorting when it is being used, and rendering times include data structure lookups along with rendering tasks like ray tracing and rasterization. For each data point, we measure the times for 100 frames and average them. The measurements are run at increments of 128 entries. They were run on a PC with an RTX 3090 GPU.

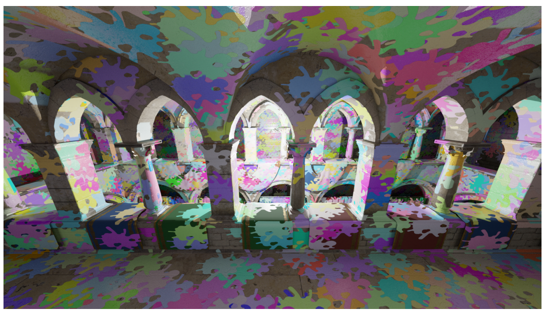
(a) Decal rendering with 65536 decals.

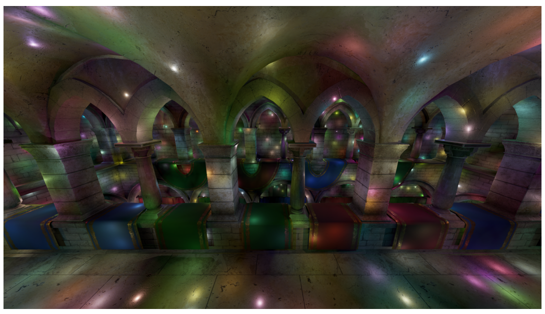
(b) Light culling with 65536 lights.

Figure 3: We use the “Sponza” scene in our measurements of both example use cases of implicit grids. We vary the number of entries from 0 to 65536. When the compared algorithms are functioning correctly, there are no differences in image quality or contents.

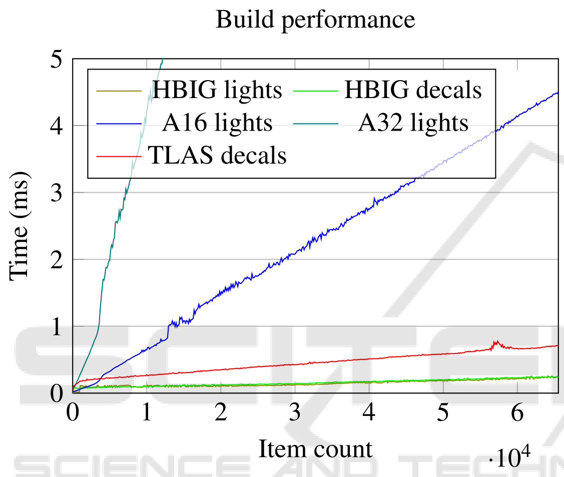

Figure 4: Performance scaling of the build step of each method as the number of entries changes.

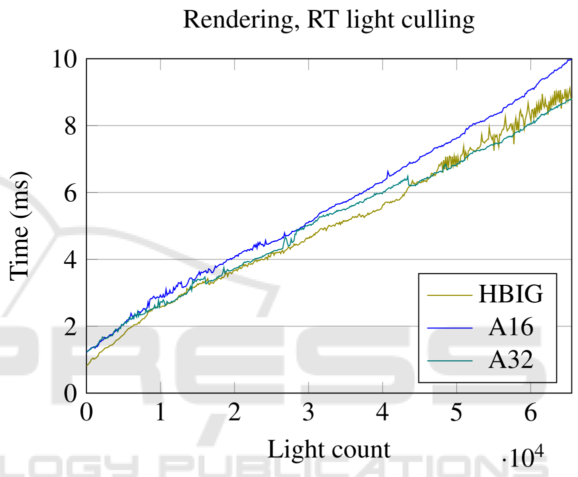

Figure 5: Performance scaling of rendering with each method in the light culling use case in ray tracing. Differences are diminished due to shadow rays being skipped for false-positive lights.

5 RESULTS

Figure 4 shows the build time of each compared data structure. The build times between ray tracing and multi-view runs are essentially identical due to the workload being the exact same, so we only present the build times measured from the ray tracing runs. At 65536 entries, implicit grids only took 0.24 ms to build in both use cases. The 32^3 3D array took around 27 ms to build, while 16^3 took $\sim$4.5 ms. Building the decal TLAS took $\sim$0.7 ms, which is around triple that of the implicit grid method.

As shown in Figure 5, there are no big differences in the rendering times between the methods when ray tracing shadow rays, other than the 16^3 3D array being slightly slower at high light counts. This slowdown is caused by light lists in each cell being larger than necessary due to the limited precision, resulting in poor culling. The differences between all of the methods are small due to shadow rays being skipped for all “false-positives”; lights that are in range according to the data structure but can still be culled based on their range limit.

In the multi-view rasterization case, we only cull lights based on the structures themselves, and do not skip “false-positives” the same way as previously. Therefore, Figure 6 demonstrates the differences achieved by better culling precision much more clearly; with high light counts, implicit grids are over twice as fast as 16^3 3D grids and over 25% faster than 32^3.

Figure 7 shows all decal rendering performance curves. In the ray tracing use case, implicit grids have a lower overhead at the low decal counts, but lose out in the high end as the TLAS case has a shallower slope. However, the TLAS method renders incorrect images near the end of the range due to many regions having more than 4 overlapping decals. This means that because the implicit grid method is actually cor-

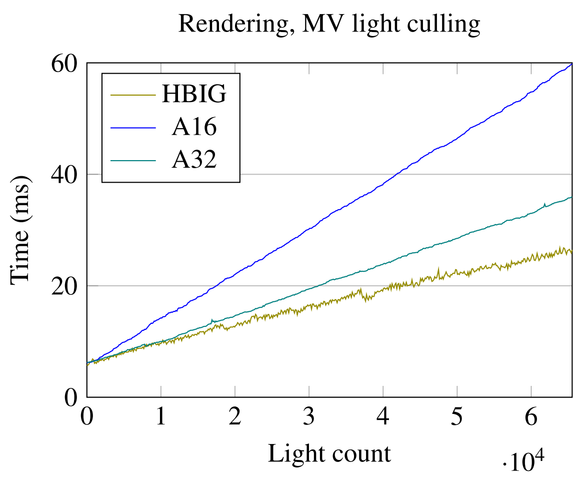

Figure 6: Performance scaling of rendering with each method in the light culling use case in multi-view rasterization. False positives are not skipped in this case, which shows the benefit of the higher precision achieved with the implicit grid.

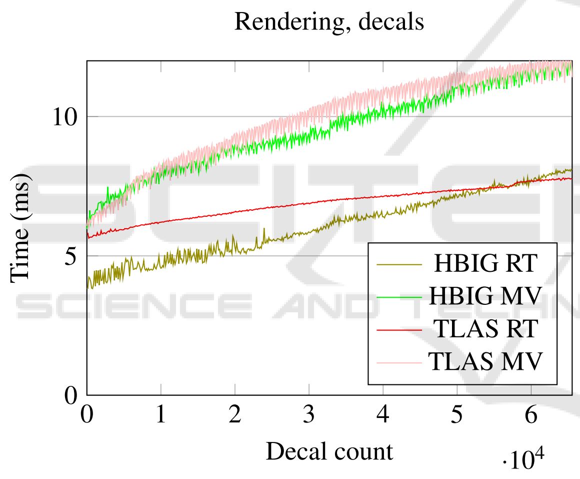

Figure 7: Performance scaling of rendering with each method in the decal rendering use case. The TLAS approach has disproportionately good results at high decal counts due to only handling up to 4 overlapping decals correctly, the rest being skipped if more decals are encountered.

rectly handling all overlapping decals, it is blending more decals together per pixel than TLAS, causing more computation and memory accesses.

The multi-view decal case shows both methods competing closely with each other in the low decal counts, with implicit grids taking a lead near 2^{14} decals. At that point, stacks of over 4 overlapping decals are rare. As the decal count increases, the TLAS method catches up to implicit grids but also starts rendering incorrect images for the same reason as in the ray tracing case.

Table 2 shows building and rendering performance differences when the hierarchy layer and sorting of entries are toggled on and off. The order of entries in the unsorted cases is random. There are only minor differences between each variation in the build times; this is expected as the workload of each build step is the same if the step is present. Rendering performance is significantly hindered if the hierarchy layer or entry sorting are disabled.

Overall, implicit grids are much faster to build than any of the other methods at practically every entry count. The rendering performance is also either similar or better than the compared methods in each situation. In total, the overall cost (build + render) of implicit grids is lower even in the TLAS comparison with ray tracing: even if we disregard TLAS's overlap issue, the build time difference of 0.47 ms to the implicit grid's benefit is enough to beat TLAS's rendering time lead of 0.36 ms at 65536 decals.

6 FUTURE WORK

Using the X, Y and Z axes for the implicit grid results in the bounding volumes being axis-aligned bounding boxes. In order to get tighter bounds around volumes which are not AABBs, more axes could be utilized, each slicing away some false positives. This would result in the bounding volumes being k-DOPs (discrete oriented polytopes).

For importance sampling of lights, it could be interesting to use an implicit-grid-like approach to represent importance trees with spatial variation. Essentially, instead of a bitmask, each slab could contain a tree structure. Then, when looking up an entry at a given point, the importance for a tree node would be dynamically constructed based on the node data in each corresponding slab. However, our cursory experiments suggest it may be challenging to find a method to preserve the sampling benefits while decoupling the tree data to slabs.

7 CONCLUSION

We presented "Hierarchical Bitmask Implicit Grids", a novel, memory-efficient spatial index data structure for querying bounding volumes based on a contained point, targeting real-time use cases on GPUs. We demonstrated the effectiveness of this data structure by applying it to both decal rendering and light culling of up to tens of thousands of decals and lights. We showed that the grid can be fully rebuilt from scratch in 0.1–2 milliseconds even with tens of thousands of entries, allowing for handling highly dynamic scenes. This build time is nearly three times

Table 2: Performance breakdown of the 65536 light culling case with ray tracing. To demonstrate the effectiveness of the hierarchy layer and entry sorting, variations of the implicit grid data structure with and without these features are listed in the table. The build time is split into 4 steps: “Sort”, “Range”, “Bitmask”, and “Hierarchy”. These refer to build steps 1, 2, 3, and 4 as listed in Section 3.2. “Render” is the time spent in ray tracing, and “Total” is the sum of all build steps and rendering time. All times are in milliseconds.

	Sort	Range	Bitmask	Hierarchy	Render	Total
Unsorted without hierarchy	N/A	0.012	0.098	N/A	25.2	25.3
Unsorted with hierarchy	N/A	0.012	0.096	0.023	30.2	30.3
Sorted without hierarchy	0.071	0.010	0.097	N/A	28.4	28.6
Sorted with hierarchy (proposed)	0.076	0.010	0.102	0.023	8.9	9.1

faster than the closest compared structure (the decal-rendering TLAS), and orders of magnitude faster than 3D arrays.

Although there is more variation in the results of our rendering performance measurements, we also demonstrate that hierarchical bitmask implicit grids can either match or exceed the compared methods in performance: At its best, our method can deliver over double the rendering performance, as seen in the multi-view light culling measurements. In the decal rendering case with ray tracing, our method gains an edge over the TLAS method due to having higher performance at lower decal counts and generating correct output at higher decal counts by not imposing a limit on overlapping decals.

Due to the positive results in the light culling and decal rendering use cases, we believe that hierarchical bitmask implicit grids could also be highly beneficial in many other GPU applications, warranting further research in various use cases.

ACKNOWLEDGEMENTS

This work was supported by the Academy of Finland under Grant 325530 and Grant 351623.

REFERENCES

Akenine-Möller, T., Haines, E., and Hoffman, N. (2018). *Real-Time Rendering*. A K Peters/CRC Press, 4th edition.

Bahnassi, W. (2021). Ray tracing decals. In *Ray Tracing Gems II: Next Generation Real-Time Rendering with DXR, Vulkan, and OptiX*, pages 427–440. Apress, Berkeley, CA.

Balestra, C. and Engstad, P.-K. (2008). The technology of Uncharted: Drake’s fortune. Game Developer Conference.

Baraff, D. (1992). *Dynamic Simulation of Non-Penetrating Rigid Bodies*. PhD thesis.

Drobot, M. (2017). Improved Culling for Tiled and Clustered Rendering. In *ACM SIGGRAPH 2017 Advances in Real-Time Rendering in Games course*.

Ericson, C. (2005). Chapter 7 - spatial partitioning. In Ericson, C., editor, *Real-Time Collision Detection*, The Morgan Kaufmann Series in Interactive 3D Technology, pages 285–347. Morgan Kaufmann, San Francisco.

Geffroy, J., Gneiting, A., and Wang, Y. (2020). Rendering the Hellscape of Doom Eternal. In *ACM SIGGRAPH 2020 Advances in Real-Time Rendering in Games course*.

Kelly, P., O’Donnell, Y., ter Elst, K., Cañada, J., and Hart, E. (2021). Ray tracing in Fortnite. In Marrs, A., Shirley, P., and Wald, I., editors, *Ray Tracing Gems II: Next Generation Real-Time Rendering with DXR, Vulkan, and OptiX*, pages 791–821. Apress, Berkeley, CA.

Looking Glass Factory, Inc. (2023). Hologram 101 - quilts. https://docs.lookingglassfactory.com/keyconcepts/key-concepts#3.-quilts. Accessed: 2023-11-14.

Morton, G. M. (1966). A computer oriented geodetic data base and a new technique in file sequencing.

Olsson, O. and Assarsson, U. (2011). Tiled shading. *Journal of Graphics*, GPU:235–251.

Olsson, O., Billeter, M., and Assarsson, U. (2012). Clustered Deferred and Forward Shading. In Dachsbacher, C., Munkberg, J., and Pantaleoni, J., editors, *Eurographics/ ACM SIGGRAPH Symposium on High Performance Graphics*. The Eurographics Association.

Sylvan, S. (2017). Thoughts on light culling for clustered shading. https://www.sebastiansylvan.com/post/light_culling/. Accessed: 2023-11-14.

The Fuchsia Authors (2021). RadixSort/VK. https://fuchsia.googlesource.com/fuchsia/+/refs/heads/main/src/graphics/lib/compute/radix_sort/. Accessed: 2023-11-14.

The Khronos Group (2018). glTF Sample Models. Accessed: 2023-11-14.

Unity Technologies (2023). Unity manual: Ray tracing light cluster. https://docs.unity3d.com/Packages/com.unity.render-pipelines.high-definition@17.0/manual/Ray-Tracing-Light-Cluster.html. Accessed: 2023-11-14.